

Electronic Supplementary Material (ESI) for Soft Matter

This journal is © The Royal Society of Chemistry 20xx

Supplementary Information

Modelling DNA extension and fragmentation in contractive microfluidic devices: a Brownian dynamics and computational fluid dynamics approach

Shuyi Wu,^a Chuang Li,^a Quanshui Zheng,^a Luping Xu^{*a}

^aCenter for Nano and Micro Mechanics, School of Aerospace Engineering, Tsinghua University, Beijing, China.

*Correspondence should be addressed to: lupingxu@tsinghua.edu.cn

Catalogue

Criteria of fragmentation.....	1
Effect of discretization degree on simulation of fragmentation	3
Two possible manners of DNA moving into an elongational flow in simulation.....	3
Two parameters to demonstrate the extension	4
DNA extension in shear flow of parameters in this study	4
Simulation of DNA extension in shear flow reported in previous experiments	5
Effect of DNA size and channel height on conformational evolution of DNA	7
Effect of accumulated fluid strain on DNA fragmentation.....	9
The first breakage site on DNA that are totally in an elongational flow.....	10
Fragmentation process of a linear-form λ DNA in a microfluidic chip.....	11

Criteria of fragmentation

A DNA molecule will be broken when stretching force acting on the molecule is larger than its tensile strength. In this study, we use this tensile strength and the corresponding critical stretching ratio as the criterion of fragmentation. Some reported studies measured the mechanical properties of single DNA molecule using optical tweezers, magnetic tweezers, atomic force microscope (AFM) and molecular combing:

Philippe Cluzel, et al[1] measured the force-displacement response of an individual duplex DNA using a tensile apparatus, and the last data point on the relation curve before breakage shows that the force is 160 pN and the stretching ratio is 1.7. As the value of force when DNA is broken could be missed in experiments, therefore the fracture strength of a single DNA molecule may be larger than 160 pN.

Matthias Rief, et al[2] measured the mechanics of single DNA molecules using AFM. The result shows that the sequence of DNA significantly influences the mechanics of DNA molecule. A λ DNA molecule transfers from B-form to S-form at 65 pN, and melts at 150 pN. The melting means that the DNA is split into single strands. For double-stranded poly (dG-dC) DNA, the B-S transition occurs at 65 pN and the melting transition occurs at 300 pN. For duplex poly(dA-dT) DNA, both the B-S transition and strands melting occur at 35 pN. The largest forces that were recorded in different tensile experiments for different DNA molecules are about 800pN, 350pN, 550pN and 500pN respectively.

D. Bensimon, et al[3] stretched DNA molecules on a surface by molecular combing[4] and calculated the tensile strength of single DNA molecules, which is 476 ± 84 pN with the corresponding stretching ratio being 2.14.

Christopher P Calderon, et al[5] measured the mechanical properties of DNA molecules by AFM. The authors reported the B-S transition and strands melting process, and the recorded largest force acting on a λ DNA molecule in tensile experiments is about 350pN.

Rupert Krautbauer, et al[6] also carried out the tensile experiment of individual DNA molecule by AFM, and both the B-S transition and strands melting were reported. After the melting at 150 pN, the double-stranded DNA become two single strands and only one strand

still attaches the tip and substrate. For this one strand, the recorded largest force in the tensile experiment is about 240 pN.

Vivek S. Jadhav, et al[7] measured force-extension curve of DNA molecules using optical tweezers, and the force-extension curve shows that the DNA ruptures at about 90pN.

Wuen-shiu Chen, et al[8] measured the force-extension curve of single-stranded synthetic DNA. The recorded largest forces for poly (dA) are 450 pN, 400 pN, 300 pN, 500 pN and 470 pN. For poly (dT), the recorded largest forces are 550 pN.

Changhong Ke. et al[9] measured the mechanics of single-stranded synthetic DNA. The recorded largest forces in tensile experiments for different single-stranded DNA are 480pN (poly(dA)), 580pN (poly(dA)), 600pN (poly(dA)), 640pN (poly(dT)), 680pN (poly(dT)) and 960 (poly(dT)).

Fig. S1 shows the tensile strength or the recorded largest force on force-extension curves of single-stranded or double-stranded DNA measured by eight reported studies. According to the experimental data, we set the tensile strength of DNA molecules in our simulation as 483 pN and the corresponding critical stretching ratio as 2.14, the former of which is almost the average of reported data.

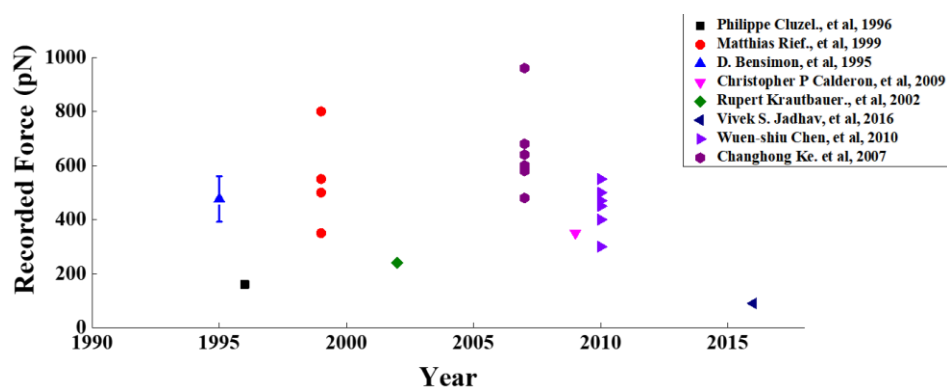


Fig. S1 The tensile strength or the recorded largest force on force-extension curves of single-stranded or double-stranded DNA measured by eight reported studies.

Effect of discretization degree on simulation of fragmentation

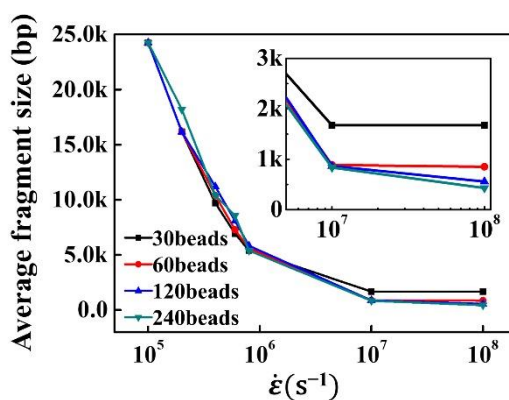


Fig. S2 Average fragment size (AFS) of a DNA molecule in elongational flow of various $\dot{\epsilon}$. The λ DNA molecule was simulated by the bead-spring model with 30, 60, 120 and 240 beads.

Two possible manners of DNA moving into an elongational flow in simulation

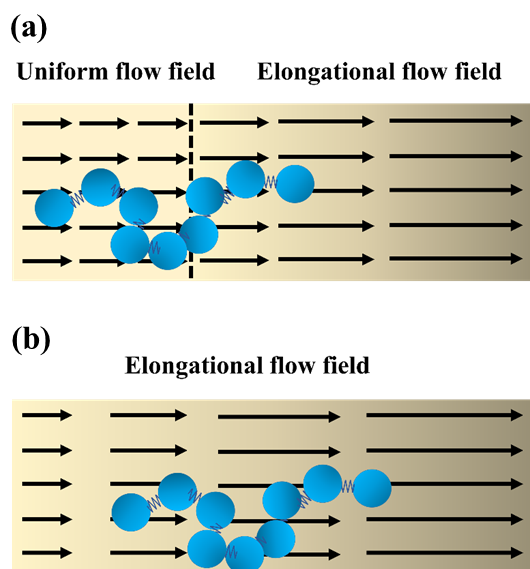


Fig. S3 The schematic diagram of two manners of DNA moving into an elongational flow. (a) DNA molecules move from a uniform flow field into an elongational flow field, which mimics the situation in realistic microfluidic channels. (b) All beads of a DNA molecule are set in the elongational flow at the beginning of simulation.

Two parameters to demonstrate the extension

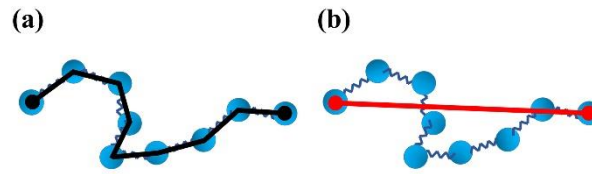


Fig. S4 Schematic diagram of two parameters to demonstrate the extension of a DNA molecule. (a) The contour length of DNA is shown with the black polyline and (b) the largest distance with the red line.

DNA extension in shear flow of parameters in this study

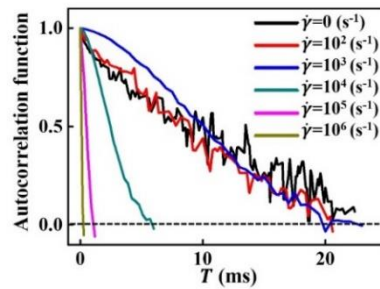


Fig. S5 Autocorrelation function $\langle \Delta LD(t)\Delta LD(t+T) \rangle / \langle \Delta LD(t)\Delta LD(t) \rangle$ as a function of the time delay T for various $\dot{\gamma}$.

Simulation of DNA extension in shear flow reported in previous experiments

A reported experiment to study dynamics of single-DNA in steady shear flow was reproduced with our BD-CFD simulation. Then, we compared the simulation results with the experimental data in term of both the transient properties and steady state of DNA molecules in shear flow. We set the solvent viscosity according to the experimental parameters to control the relaxation time of DNA molecules and to reproduce the experimental condition. The visually recorded “extension” of DNA in the reported experimental results is represented as the largest distance in our simulation work.

(1) Transient properties of DNA in shear flow

Fig. S6 shows the conformational evolution of an individual DNA molecule in shear flow of three shear rates, which agree well with the experimental result (see Fig. 2 in Ref.[10]) in term of the level of extension and the frequency of fluctuation in DNA extension for shear flow with different shear rate. The time scale of DNA transient evolution in shear flow can be quantitatively analyzed by the autocorrelation function of contour length. The simulated relationship between the autocorrelation function and accumulative flow strain (Fig. S7) agrees well with the experimental data (see Fig. 6c in Ref.[10]).

(2) Steady state of DNA in shear flow

Probability distributions of the largest distance for DNA molecules that have arrived steady state in several shear flow conditions (Fig. S8) aligns well with the experimental results (see Fig. 5 in Ref.[10]).

These results show that our BD-CFD method is valid to simulate both the transient properties and steady state of DNA molecules in shear flow.

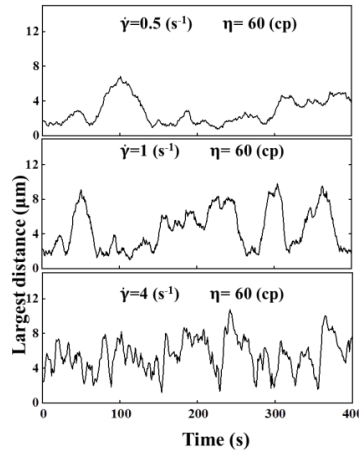


Fig. S6 Evolution of the largest distance for an individual λ DNA in shear flow of different shear rates. The relaxation time of the DNA is controlled by setting the solvent viscosity $\eta = 60$ centipoise.

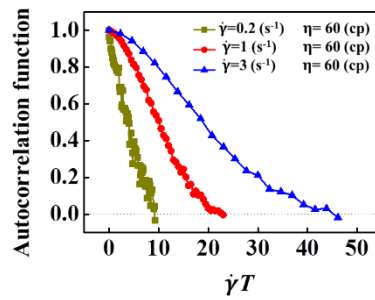


Fig. S7 Autocorrelation function of the largest distance, $\langle \Delta LD(t)\Delta LD(t+T) \rangle / \langle \Delta LD(t)\Delta LD(t) \rangle$, as a function of the accumulative flow shear strain, $\dot{\gamma}T$.

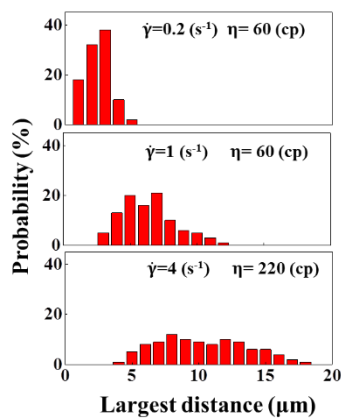


Fig. S8 Probability distributions of the largest distance for DNA in shear flow of different shear rates and solvent viscosities. The data size for each flow condition is 100 DNA molecules that have arrived steady state.

Effect of DNA size and channel height on conformational evolution of

DNA

In order to analyze the conformation distributions of DNA in micro-channels, we simulated the extension of DNA molecules of different sizes in micro-channels of different heights. The channels' heights (H) is set according to reported microfluidic chips, *i.e.* 10, 25, 50 and 200 μm , respectively. The flow rate is set as 1 ml/min and the width of channels is 200 μm . We simulated DNA molecules of five different sizes, namely 8, 24, 48, 96 and 192Kbp. For every simulation condition with a combination of DNA size and channel height, we chose 25 initial locations in a quarter area of the inlet section of the micro-channel and put 10 DNA molecules in every initial location to simulate DNA conformational evolution. Therefore, the data size for every condition is 250 DNA molecules. Due to the distribution of flow velocity in a channel (faster at the center and slower near the walls), more DNA molecules move through the center of a channel than those move near walls. When we calculate the conformation distribution of DNA molecules in the whole channel, we give weight coefficients to the molecules, which is proportional to the local flow velocity at the initial locations of the DNA molecules.

In term of the effect of channel height on conformational evolution of DNA, the result shows that as the channel height decreases, the conformation distributions of DNA moving near the walls have a significantly change and the percentage of linear DNA increases from 52% ($H = 200 \mu\text{m}$) to 70% ($H = 10 \mu\text{m}$) (see Fig. S9). Meanwhile, the conformation distributions of DNA moving near the center of the micro-channel are almost unchanged, because the shear rates near the center of all channels are always very small, although the shear rate near walls significantly increases with the channel height decreasing. Moreover, as the flow velocity near the center of channels is larger than that near the walls, most DNA molecules move through the center at the same time period. Therefore, the integrated conformation distributions of DNA in channels of different heights are similar with each other (Fig. S10).

In term of the effect of DNA size on conformational evolution, the result shows that as the size of DNA increases, the percentage of coiled conformation decreases (Fig. S10). This is

because that it is difficult for large DNA to relax back to a coiled conformation in shear flow and large DNA molecule suffers larger shear force than small one. Moreover, for the largest DNA molecules (192Kbp), it is difficult to keep complete linear conformation, and therefore the percentage of linear conformation is less than that of shorter DNA. For long DNA molecules (192Kbp), more possible conformations can be observed during the conformational evolution in shear flow (Fig. S11) and few 192Kbp DNA molecules that move near walls of the micro-channel are fragmented by strong shear flow (6.4% for $H = 25\mu\text{m}$ and 11.2% for $H = 10\mu\text{m}$).

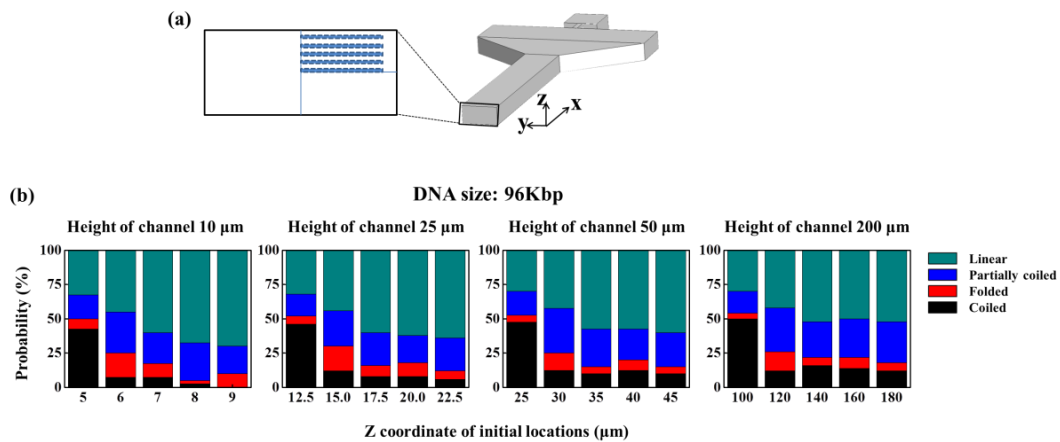


Fig. S9 Conformation Distributions of DNA molecules that move at different locations of micro-channels of different heights. For every micro-channel, the DNA locations are classified into five groups by the Z coordinate of initial locations. The size of DNA molecules is 96Kbp. The height of the four micro-channels are 10, 25, 50 and 200 μm .

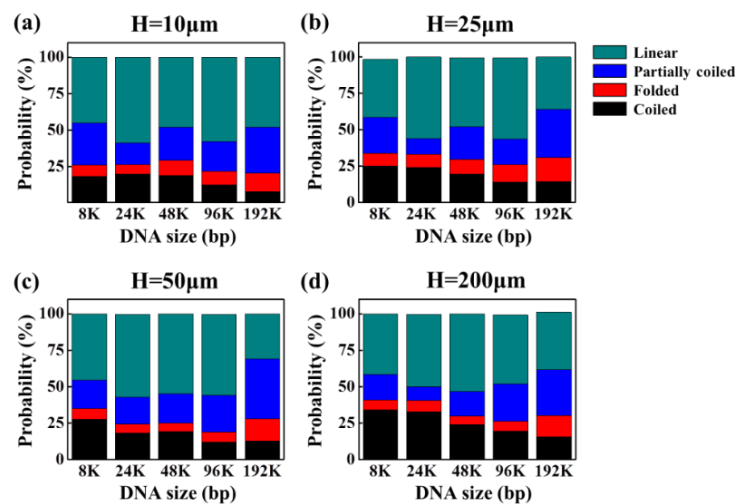


Fig. S10 The conformation distributions of different DNA molecules in micro-channels of different heights. The heights of channels for panel a-d are 10, 25, 50 and 200 μm , respectively.

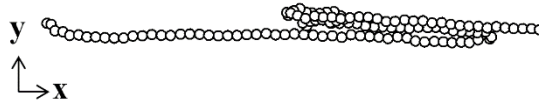


Fig. S11 Another kind of possible conformations of long DNA molecules evolved in micro-channel. The size of this DNA molecule is 192Kbp, and the height of channel is 50 μ m. To clearly show the conformation, the scale of the y direction is two time that of the x direction. This kind of DNA conformations is classified as folded DNA.

Effect of accumulated fluid strain on DNA fragmentation

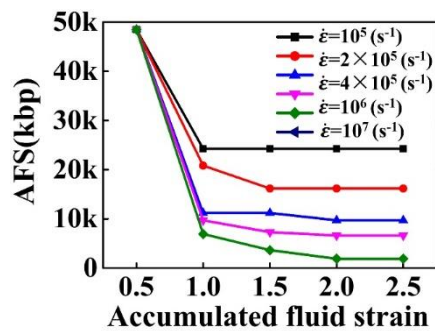


Fig. S12 Relationship between average fragment size and accumulated fluid strain with various strain rate. The initial velocity of the elongational flow is set as 4m/s. The initial conformation of DNA is linear with the stretching ratio set one.

The first breakage site on DNA that are totally in an elongational flow

We simulated the fragmentation of DNA molecules that are set in a uniform elongational flow with uniform strain rate when the simulation begins, and analyzed the distribution of the first breakage site (see Fig. S13). The result shows that in weak elongational flow ($\dot{\epsilon} = 10^5 \text{ s}^{-1}$), most linear DNA molecules break near the middle of DNA. As the strain rate increase from 2×10^5 to $6 \times 10^5 \text{ s}^{-1}$, the distribution of the first fragmentation site becomes broader with an obvious peak of the distribution at the midpoint of DNA. In elongational flow with higher strain rate ($\dot{\epsilon} = 10^7 \text{ s}^{-1}$), the peak disappears and the distribution shows an obvious uniform distribution near the middle of DNA.

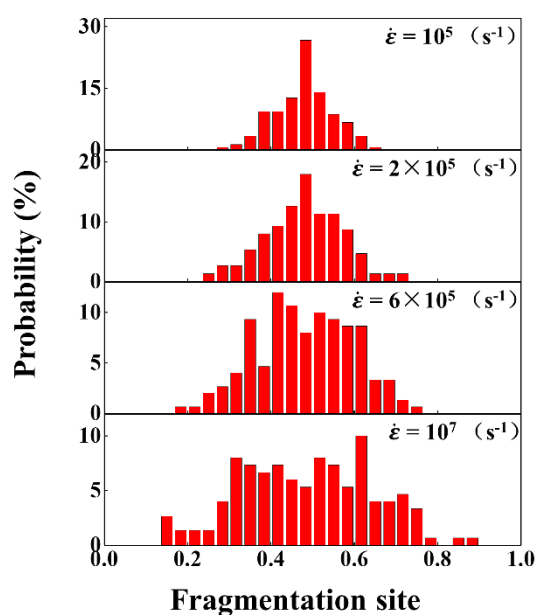


Fig. S13 Distributions of the first fragmentation sites for linear DNA in elongational flow with different strain rate. DNA molecules are set in the elongational flow at the beginning of simulation. The length of DNA is normalized and the end of DNA labeled by zero is the front end. The linear DNA are chosen from DNA molecules evolved in a shear flow of $\dot{\gamma} = 10^6 \text{ s}^{-1}$, and the data size of linear DNA is 150.

Fragmentation process of a linear-form λ DNA in a microfluidic chip

We analyzed the fragmentation process of a linear-form λ DNA in a contractive microfluidic chip (Fig. S14a). The distribution of strain rate in the contractive area is shown in Fig. S14b. As the DNA moves in the elongational flow area, DNA is fragmented at where the drag force is high enough rather than at the midpoint of the DNA molecule, such as at fragmentation site ① in Fig. S14c, site ③ in Fig. S14e, site ④ in Fig. S14f, site ⑦ in Fig. S14i and site ⑧ in Fig. S14j. Because the local strain rates at these fragmentation sites are lower than that near the corner, the size of these DNA fragments are large. Then, as these large DNA fragments keep moving, they break again at areas of higher strain rate, such as at fragmentation site ② in Fig. S14d, site ⑤ in Fig. S14g, site ⑥ in Fig. S14h and site ⑨ in Fig. S14k. The results also indicate that fragmentation occurs when stretching force is high enough to break DNA, which is different from the reported “midpoint-breakage” phenomenon.

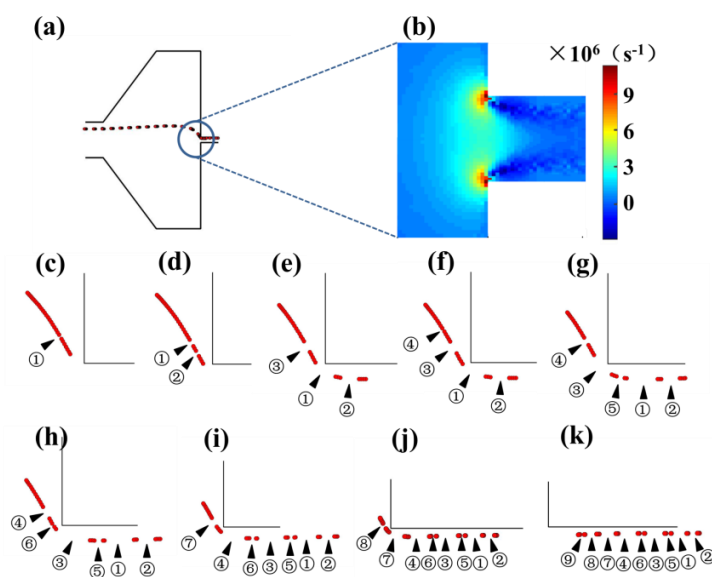


Fig. S14 Fragmentation process of a λ DNA with linear conformation in a contractive microfluidic chip. (a) Schematic diagram of a DNA fragmented in a microfluidic chip. (b) The distribution of strain rate at the contractive area of the micro-channel. Structure parameters of the microfluidic chip are shown in Figure 1a and the flow rate is 4ml/min. (c-k) Fragmentation process and fragmentation sites on a λ DNA molecule when it moves through the elongational flow area. The fragmentation sites are highlighted with black triangles and the sequence of fragmentation site is labeled by numbers.

Reference

- [1] Cluzel P, Lebrun A, Heller C, Lavery R, Viovy J L, Chatenay D and Caron F 1996 DNA: an extensible molecule *Science* **271** 792-4
- [2] Rief M, Clausen-Schaumann H and Gaub H E 1999 Sequence-dependent mechanics of single DNA molecules *Nature Structural Biology* **6** 346-9
- [3] Bensimon D, Simon A J, Croquette V V and Bensimon A 1995 Stretching DNA with a receding meniscus: Experiments and models *Phys Rev Lett* **74** 4754-7
- [4] Bensimon A, Simon A, Chiffaudel A, Croquette V, Heslot F and Bensimon D 1994 Alignment and sensitive detection of DNA by a moving interface *Science* **265** 2096-8
- [5] Calderon C P, Chen W H, Lin K J, Harris N C and Kiang C H 2009 Quantifying DNA melting transitions using single-molecule force spectroscopy *J Phys Condens Matter* **21** 34114
- [6] Krautbauer R, Pope L H, Schrader T E, Allen S and Gaub H E 2002 Discriminating small molecule DNA binding modes by single molecule force spectroscopy *FEBS Lett* **510** 154-8
- [7] Jadhav V S, Bruggemann D, Wruck F and Hegner M 2016 Single-molecule mechanics of protein-labelled DNA handles *Beilstein J Nanotechnol* **7** 138-48
- [8] Chen W S, Chen W H, Chen Z, Gooding A A, Lin K J and Kiang C H 2010 Direct observation of multiple pathways of single-stranded DNA stretching *Phys Rev Lett* **105** 218104
- [9] Ke C, Humeniuk M, H S G and Marszalek P E 2007 Direct measurements of base stacking interactions in DNA by single-molecule atomic-force spectroscopy *Phys Rev Lett* **99** 018302
- [10] Smith D E, Babcock H P and Chu S 1999 Single-polymer dynamics in steady shear flow *Science* **283** 1724-7